PLOS | ONE

RESEARCH ARTICLE

Serum uPAR as Biomarker in Breast Cancer Recurrence: A Mathematical Model

Wenrui Hao[1]*, **Avner Friedman**[1,2]

1 Mathematical Biosciences Institute, The Ohio State University, Columbus, OH, United States of America, **2** Department of Mathematics, The Ohio State University, Columbus, OH, United States of America

* hao.50@mbi.osu.edu

Abstract

There are currently over 2.5 million breast cancer survivors in the United States and, according to the American Cancer Society, 10 to 20 percent of these women will develop recurrent breast cancer. Early detection of recurrence can avoid unnecessary radical treatment. However, self-examination or mammography screening may not discover a recurring cancer if the number of surviving cancer cells is small, while biopsy is too invasive and cannot be frequently repeated. It is therefore important to identify non-invasive biomarkers that can detect early recurrence. The present paper develops a mathematical model of cancer recurrence. The model, based on a system of partial differential equations, focuses on tissue biomarkers that include the plasminogen system. Among them, only uPAR is known to have significant correlation to its concentration in serum and could therefore be a good candidate for serum biomarker. The model includes uPAR and other associated cytokines and cells. It is assumed that the residual cancer cells that survived primary cancer therapy are concentrated in the same location within a region with a very small diameter. Model simulations establish a quantitative relation between the diameter of the growing cancer and the total uPAR mass in the cancer. This relation is used to identify uPAR as a potential serum biomarker for breast cancer recurrence.

Citation: Hao W, Friedman A (2016) Serum uPAR as Biomarker in Breast Cancer Recurrence: A Mathematical Model. PLoS ONE 11(4): e0153508. doi:10.1371/journal.pone.0153508

Editor: Yi-Hsien Hsieh, Institute of Biochemistry and Biotechnology, TAIWAN

Received: December 10, 2015

Accepted: March 30, 2016

Published: April 14, 2016

Data Availability Statement: All relevant data are within the paper.

Funding: The authors have been supported by the Mathematical Biosciences Institute and the National Science Foundation under Grant DMS 0931642.

Competing Interests: The authors have declared that no competing interests exist.

Introduction

Human breast cancer is a major cause of death in the United States and worldwide [1]. It is estimated that 230,000 women in the United States are diagnosed annually with invasive breast cancer, and more than 40,000 die from the disease [2]. A major factor that contributes to poor prognosis is the fact that diagnosis is often delayed due to limitation in mammography screening [3]. Poor prognosis occurs also in assessing the risk of recurrence in patients of low grade breast cancer; improving this assessment will help avoid unnecessary chemotherapy [4].

Risk factors associated with gene mutations such as BRCA1 and BRCA2, and with family history and aging have long been recognized [5]. More recent work is also looking for risk assessment that can be associated with serum biomarkers [6–8]. Three tissue biomarkers have been identified: urokinase plasminogen activator (uPA), plasminogen-activator-inhibitor

(PAI-1), and tissue factor (TF) [3, 4, 9, 10]. For uPA to become active it must bind to its receptor uPAR [11]. Active uPA is extracellular matrix-degrading protease that promotes tumor progression and metastasis. It binds to plasminogen and converts it to its activated form, plasmin, a process inhibited by PAI-1 [12–16]. Plasmin mediates the activation of matrix metaloproteinase (MMP) which enables cancer cells' migration [12, 15, 17]. TF promotes tumor by enhancing VEGF production [18]. Harbeck et. al [19] reported on an extensive 6-year study to assess the risk associated with node-negative breast cancer recurrence in terms of the levels of uPA and PAI-1. Based on this report and other studies it was concluded that tissue (uPA, PAI-1) provide predictive information about early breast cancer [4, 20]. The American Society of Clinical Oncology also recommends uPA and PAI-1 as prognostic tumor markers for breast cancer [21].

Although uPA and PAI-1 levels are elevated in breast cancer tissue, these high levels are not detected in the blood. Indeed, as reported in Rha et al.[22], the blood level of uPA and PAI-1 of the plasminogen activation system correlated with that of breast tissue in order of $R^2 = 0.35$ for uPA and $R^2 = 0.11$ for PAI-1. So uPA and PAI-1 are not reliable serum biomarkers. On the other hand, it was reported by Rha et al. [22], that the correlation of the level of uPAR in the blood with that of tissue is significant, with $R^2 = 0.61$ (P = 0.001). Recently Soydine et al. [23] found that uPAR in serum and in urine of breast cancer patients (n = 180) was significantly higher than in healthy control (n = 60). Serum uPAR was also shown to be a prognostic biomarker in endometrial cancer [24].

The present paper is concerned with prognosis of breast cancer recurrence. Most commonly, recurrence occurs within 3–5 years, although the statistics of recurrence is not clear [25, 26]. When breast cancer recurs, it most often recurs in the same location as the primary cancer [27]. In the present paper we address with a mathematical model the following question: Can uPAR be used as biomarker to recognize breast cancer recurrence? We assume that after treatment of the original cancer, some cancer cells survived in the same location, occupying a small spherical region of radius R_0 and that the cancer begins to grow while maintaining a spherical shape. Simulations of our mathematical model profile the cancer radius and the expression of uPAR as functions of R_0 and time t: $R(R_0, t)$ and $uPAR(R_0, t)$. If a patient's uPAR in tissue (surrounding the primary tumor) is measured at time t, say at $t = 100$ days, we can then use this measurement to determine R_0 and hence also the tumor radius $R(R_0, t)$ for any time t after 100 days. The articles of Rha et al. [22] and Soydine et al. [23] suggest that the uPAR level in serum is siginificantly correlated and hence proportional to the level of uPAR in the tissue, hence serum uPAR could serve as a potential biomarker. When clinical data become available to more reliably confirm this proportionality coefficient, the uPAR could then actually be used as serum biomarker for breast cancer recurrence.

Model

The mathematical model is based on the diagram shown in Fig 1. The model includes, in addition to uPA, uPAR and PAI-1, also TF, VEGF, M-CSF, MMP and MCP-1. It also includes the cells that produce these proteins, or activated by them, namely cancer cells, fibroblasts, macrophages and endothelial cells. The variables of the model are listed in Table 1. The model is described by a system of partial differential equations (PDEs) in a radially symmetric tumor, with evolving radius $R(t)$. The initial radius, $R_0 = R(0)$, is a parameter which is patient-dependent. We shall assume that the total density of cells at each point in the tissue is constant; since tumor cells proliferate, the radius $R(t)$ is increasing with time and cells are moving with velocity $\mathbf{u}$ which is time dependent.

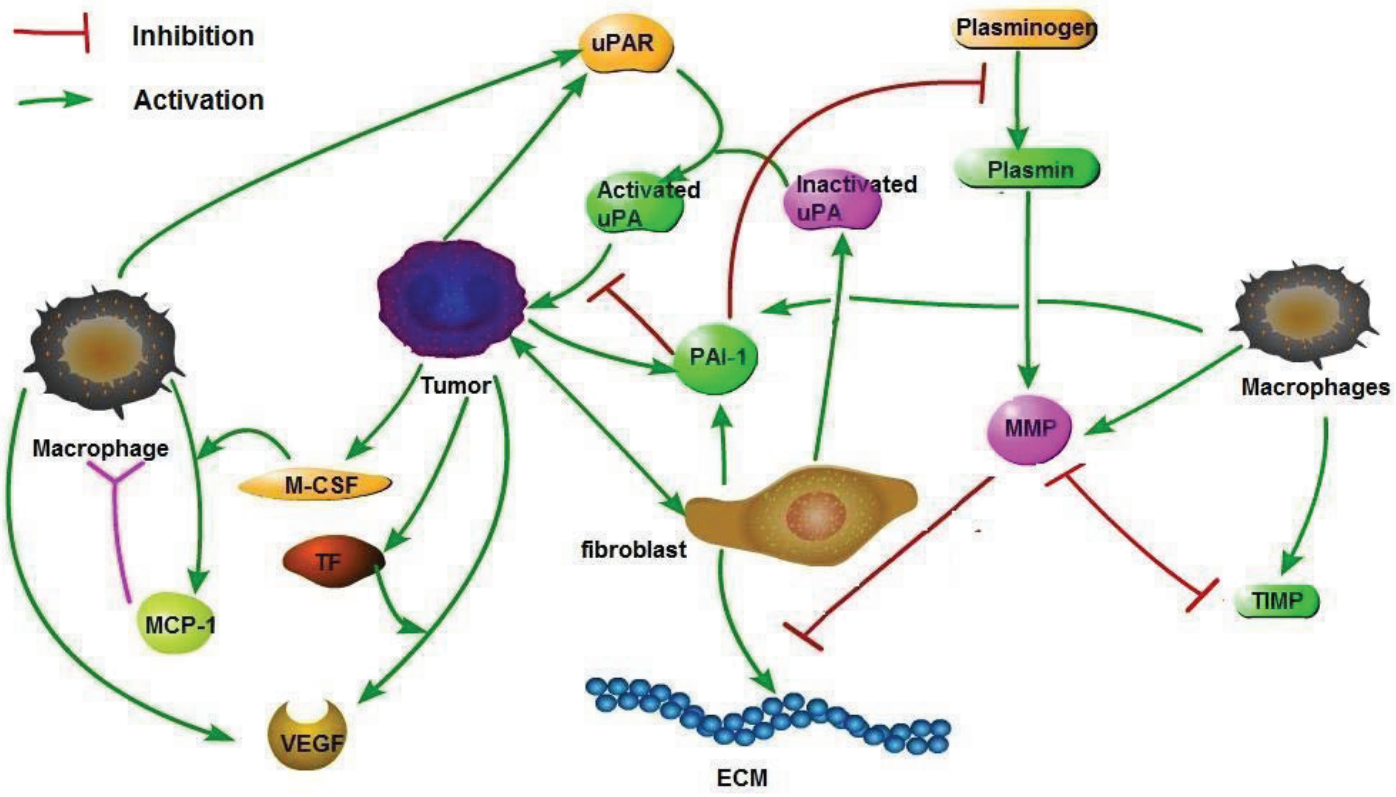

Fig 1. Schematic network of breast cancer with uPA, PAI-1 and uPAR: Arrows means activation; block arrow means inhibition.

doi:10.1371/journal.pone.0153508.g001

Table 1. The variables of the model; concentration and densities are in units of g/cm^3.

T:	concentration of tissue factor	V:	concentration of VEGF
P:	concentration of plasmin	u_{PR}:	concentration of uPAR
u_P^i:	concentration ofinactivated uPA	u_P^a:	concentration of activated uPA
P_A:	concentration of PAI-1	q:	concentration of M-CSF
p:	concentration ofMCP-1	M:	macrophage density
E:	endothelial cell density	T_β	TGF-β concentration
G:	EGF concentration	f:	fibroblast density
C:	cancer cell density	w:	concentration of oxygen
Q:	concentration of MMP	Q_r:	concentration of TIMP
ρ:	ECM density	$R(t)$:	radius of tumor at time t
$\mathbf{u}$:	cell velocity		

doi:10.1371/journal.pone.0153508.t001

Equation for tissue factor (T)

The tissue factor equation is given by

$$\frac{\partial T}{\partial t} - D_T \Delta T = \underbrace{A_T + \lambda_{TC} C}_{production} \underbrace{-d_T T}_{degradation}, \quad (1)$$

where the second term is the production by cancer cells [28, 29].

Equation for VEGF (V)

The evolution of VEGF concentration is modeled by

$$\frac{\partial V}{\partial t} - D_V \Delta V = \underbrace{\lambda_{VC} C(1 + \lambda_{VT} \frac{T}{K_T + T}) + \lambda_{VM} M}_{activation} \underbrace{-d_V V}_{degradation}. \quad (2)$$

The first term on the right-hand side accounts for production of VEGF by cancer cells [28, 30, 31], a process enhanced by tissue factor [18], and the second term accounts for VEGF produced by macrophages [30, 31].

Equation for plasmin (P)

Plasminogen is the inactive precursor of trypsin-like serine plasmin. When it becomes activated, it is converted to plasmin. The generation of plasmin requires the binding of uPA to plasminogen, after uPA was released from the complex uPA-uPAR and became active [32], and this binding is inhibited by PAI-1 [12–16]. For simplicity we take the concentration of plasminogen to be constant. Hence the concentration of plasmin concentration satisfies the equation

$$\frac{\partial P}{\partial t} - D_P \Delta P = \underbrace{\lambda_P (1 + \lambda_{Pu} \frac{u_P^a}{K_{P_A} + P_A})}_{production} \underbrace{-d_P P}_{degradation}. \quad (3)$$

Equation for uPAR (u_{PR})

The uPA receptor uPAR is expressed by macrophages [11, 33] and breast cancer cells [34]. Hence the equation of uPAR can be written as follows:

$$\frac{\partial u_{PR}}{\partial t} - D_{u_{PR}} \Delta u_{PR} = \underbrace{\lambda_{u_{PR}M} M + \lambda_{u_{PR}C} C}_{production} \underbrace{-d_{u_{PR}} u_{PR}}_{degradation}. \quad (4)$$

Equation for uPA (u_P^i and u_P^a)

Inactive uPA is produced by fibroblasts [35]. Hence,

$$\frac{\partial u_P^i}{\partial t} - D_{u_P} \Delta u_P^i = \underbrace{\lambda_{uf} f}_{production} \underbrace{-d_{u_P^i} u_P^i}_{degradation}. \quad (5)$$

uPA is activated when inactive uPA combines with uPAR. We take the equation for u_P^a to be

$$\frac{\partial u_P^a}{\partial t} - D_{u_P} \Delta u_P^a = \underbrace{\lambda_u u_P^i \frac{u_{PR}}{K_{u_{PR}} + u_{PR}}}_{production} \underbrace{-d_{u_P^a} u_P^a}_{degradation}. \quad (6)$$

Equation for PAI-1 (P_A)

The equation of the PAI-1 concentration is given by

$$\frac{\partial P_A}{\partial t} - D_{P_A}\Delta P_A = \underbrace{\lambda_{PC}C + \lambda_{Pf}f + \lambda_{PM}M}_{production} \underbrace{-d_{P_A}P_A}_{degradation}. \tag{7}$$

The first three terms on the right-hand side account for production of PAI-1 by cancer cells [11], fibroblasts [11, 36] and macrophages [37].

Equation for M-CSF (q)

The M-CSF concentration satisfies the equation

$$\frac{\partial q}{\partial t} - D_q\Delta q = \underbrace{\lambda_{qC}C}_{production} \underbrace{-d_q q}_{degradation}, \tag{8}$$

where the first term of the right-hand side account for production by cancer cells [38].

Equation for MCP-1 (p)

The equation of the MCP-1 concentration is given by

$$\frac{\partial p}{\partial t} - D_p\Delta p = \underbrace{\lambda_p(w)\frac{q}{q_0+q}M}_{production} \underbrace{-d_p p}_{degradation}. \tag{9}$$

The first term of the right-hand side accounts for production of MCP-1 by macrophages activated by M-CSF [31, 39]. Here $\lambda_p(w) = \lambda_p \frac{w}{w_h}$ if $w < w_h$ and $\lambda_p(w) = \lambda_p$ if $w > w_h$, where w_h is an appropriate hypoxic level.

Equation for macrophages (M)

We assume that all cells are moving with common velocity $\mathbf{u}$, and are subject to dispersion. The equation of macrophages density is given by

$$\frac{\partial M}{\partial t} + \nabla\cdot(\mathbf{u}M) - D_M\Delta M = \underbrace{\beta\frac{p}{K_p+p}M_0}_{source} \underbrace{-\nabla(\chi_C M\nabla(p))}_{chemotaxis} \underbrace{-d_M M}_{death}, \tag{10}$$

where D_M is the dispersion coefficient. The second term of the right-hand side accounts for chemotaxis [28, 31, 39]. Monocytes from the vascular system, with density M_0, are attracted to the tissue by MCP-1, and they differentiate into macrophages. Macrophages are terminally differentiated cells. On the boundary of each blood vessel within the tumor there holds a flux condition, which we take to be

$$\frac{\partial M}{\partial n} - \widetilde{\alpha_M}\frac{p}{K_p+p}M_0 = 0, \textit{forsome } \widetilde{\alpha_M} > 0.$$

As in [40] we can use a homogenization method to replace these fluxes by an average source of macrophages within the tissue, and this is the first term on the right-hand side of Eq (11). We assume that the macrophages are primarily tumor-associated-macrophages (TAM) of M2 phenotype.

Equation for endothelial cells (*E*)

Endothelial cells are chemoattracted by VEGF and their proliferation is increased by VEGF [31]. The equation for endothelial density is given by

$$\frac{\partial E}{\partial t} + \nabla \cdot (\mathbf{u}E) - D_E \Delta E = \underbrace{-\nabla(\chi_C E \nabla(V))}_{chemotaxis} \underbrace{+\lambda_E E(1 - \frac{E}{K_E})(V - V_0)^+}_{proliferation} \underbrace{-d_E E}_{death}. \quad (11)$$

where we used the notation: $X^+ = X$ if $X > 0$, $X^+ = 0$ if $X \leq 0$. The second term on the right-hand side assumes a threshold V_0 below which proliferation of E does not occur [41, 42].

Equation for fibroblasts (*f*)

There is a mutual enhancement in the interaction between cancer cells and fibroblasts. Cancer cells secrete TGF-β which increases the activation and proliferation of fibroblasts, while EGF secreted by fibroblasts increases the proliferation of cancer cells [43–50].

We write simplified equations for TGF-β (T_β) and EGF(G):

$$\frac{dT_\beta}{dt} = \lambda_{T_\beta} C - d_{T_\beta} T_\beta, \qquad \frac{dG}{dt} = \lambda_G f - d_G G.$$

The growth of cancer cells occurs on a time scale of days, whereas the secretion and decay of cytokines occur on a time scale of minutes to hours [51]. In order to understand the growth of cancer we simplify the model by using quasi-steady-state approximation for the equations of T_β and E, so that $T_\beta = c_1 C$, $G = c_2 f$ for some constants c_1 and c_2. Then the fibroblasts-enhanced growth rate of fibroblast density (f) through T_β may be replaced by $\lambda_{fC} C$, and the tumor-cell-enhanced proliferation of cancer density (C) through G may be replaced by $\lambda_{Cf} f$. We use the Michaelis-Menten law to express the enhanced proliferation of fibroblasts by T_β (i.e., by $c_1 C$) because TGF-β activation of fibroblast and EGF enhancement of cancer cells may be limited due to the limited rate of receptors recycling associated with this process.

The equation of fibroblast density is then given by

$$\frac{\partial f}{\partial t} + \nabla \cdot (\mathbf{u}f) - D_f \Delta f = \underbrace{A_f + \lambda_{fC} f \frac{C}{K_C + C}}_{proliferation} \underbrace{-d_f f}_{death}. \quad (12)$$

Equation for cancer cells (C)

The equation of the cancer cells density is given by

$$\frac{\partial C}{\partial t} + \nabla \cdot (\mathbf{u}C) - D_C \Delta C = \underbrace{\left[\lambda_C(w) + \lambda_{Cf}\frac{f}{K_f + f} + \lambda_{Cu_P}\frac{u_P^a}{K_{P_A} + P_A}\frac{u_{PR}}{K_{u_{PR}+u_{PR}}}\right] C\left(1 - \frac{C}{C_0}\right)}_{proliferation} \underbrace{-d_C C}_{death}. \quad (13)$$

There are three terms in the bracket: The first term is for tumor growth at rate which is oxygen dependent; the second term represents enhancement by EGF produced by fibroblasts; the third term accounts for proliferation of cancer cells by uPA as it binds to its receptor uPAR on cancer cells [11, 12, 15, 36], a process resisted by PAI-1 [14, 16]. The Michaelis-Menten law is used to represent the limited rate of receptor recycling associated with the enhancements by f and by u_{PR}. We take $\lambda_C(w) = \lambda_{wC}\frac{w}{w_h}$ if $w \leq w_h$ and $\lambda_C(w) = \lambda_{wC}$ if $w \geq w_h$.

Equation for oxygen (w)

The oxygen concentration evolves according to the equation

$$\frac{\partial w}{\partial t} - D_w \Delta w = \lambda_w E - d_{wM} wM - d_{wC} wC - d_{wf} wf. \quad (14)$$

The first term of the right-hand side accounts for infusion of oxygen through the blood, which is represented by the density of endothelial cells. The last three terms represent oxygen taken up by macrophages, tumor cells and fibroblasts.

Equations for MMP (Q) and TIMP (Q_r)

We have the following sets of reaction-diffusion equations for MMP and TIMP:

$$\frac{\partial Q}{\partial t} - D_Q \Delta Q = \underbrace{\lambda_{QM} M\left(1 + \lambda_{QP}\frac{P}{K_P + P}\right)}_{production} \underbrace{-d_{QQ_r} Q_r Q}_{depletion} \underbrace{-d_Q Q}_{degradation} \quad (15)$$

$$\frac{\partial Q_r}{\partial t} - D_{Q_r} \Delta Q_r = \underbrace{\lambda_{Q_r M} M}_{production} \underbrace{-d_{Q_r Q} Q Q_r}_{depletion} \underbrace{-d_{Q_r} Q_r}_{degradation} \quad (16)$$

MMP and TIMP are activated by macrophages [52, 53] and MMP activation is enhanced by plasmin P[17], and MMP is lost by binding with TIMP, while TIMP is depleted as it blocks MMP [38, 54, 55].

Equation for ECM (ρ)

Extracelluar matrix (ECM) is produced by fibroblasts [40], and is degraded by MMP [38, 54]. The equation for the density of ECM is given by

$$\frac{\partial \rho}{\partial t} + \nabla \cdot (\mathbf{u}\rho) = \underbrace{\lambda_{\rho f} f (1 - \frac{\rho}{\rho_0})^+}_{production} \underbrace{-d_\rho \rho - d_{\rho Q} Q \rho}_{degradation}, \tag{17}$$

Equation for u

We assume that the total density of all the cells plus the density of ρ is constant:

$$M + E + f + C + \rho = \text{const.} = 1. \tag{18}$$

We also assume that all cells are approximately of the same volume and surface area, so that the dispersion coefficients of the all cells have the same coefficient, D. By adding Eqs (11)–(14) and (17), we get an equation for $\nabla \cdot \mathbf{u}$:

$$\nabla \cdot \mathbf{u} + D\Delta\rho = \sum [\text{RHS of Eqs}\,(11),\,(12),\,(13),\,(14)\,\text{and}\,(17)], \tag{19}$$

We can, conversely, derive Eq (18) from Eqs (11)–(14) and (19).

We assume that if a breast cancer recurs, it is because some cancer cells survived in the initial location. We also assume, to simplify the computations, that these cells are contained in a sphere of small radius R_0, and that as time increases the region containing the cancer cells is a sphere with increasing radius $r = R(t)$, and all the model variables are radially symmetric, that is, they are functions of (r, t) where $0 \le r \le R(t)$, $t > 0$. In particular,

$$\mathbf{u} = u(r, t)\mathbf{e}_r$$

where $\mathbf{e}_r = \frac{\mathbf{x}}{|\mathbf{x}|}$ is the radial unit vector.

The free boundary equation

We assume that the tumor is spherical with radius $r = R(t)$, so that

$$\frac{dR}{dt} = \mathbf{u}\mathbf{e}_r = u(R(t), t), \tag{20}$$

where $\mathbf{e}_r = \frac{\mathbf{x}}{|\mathbf{x}|}$ is the radial unit vector.

Boundary conditions

We assume flux boundary conditions due to oxygen transport of the form

$$\frac{\partial X}{\partial \mathbf{n}} + \alpha_X (X - X_0)^+ = 0 \tag{21}$$

for $X = w$ and E, where X_0 is the density of oxygen or of endothelial cells within the vascular system at the boundary of the tumor. The coefficients α_X on the free boundary are chosen as follows: $\alpha_w = \widetilde{\alpha_w} \frac{E}{K_E + E}$, and $\alpha_E = \widetilde{\alpha_E} \frac{V}{K_V + V}$. We assume no-flux boundary condition for all other variables except ρ. Since ρ satisfies the hyperbolic Eq (17) with ue_r as the velocity of the free boundary, we do not need to prescribe a boundary condition for ρ on the free boundary. The radial velocity is determined from Eq (19).

Initial conditions

We choose the following initial conditions for ECM, oxygen and cells concentration in unit of g/cm^3: $\rho = 0.02$, $w = w_h$, $M = 0.07$, $E = 0.05$, $f = 0.06$, and $C = 0.4$. All the cytokines are taken to be initially zero. The initial conditions do not affect the simulation results after a few weeks. However, as will be shown, the very small value of $R(0)$ plays a critical role in the tumor growth profile.

Results

In Figs 2 and 3 we take $R(0) = 10^{-2}$ cm = $100\mu m$; at this initial size the tumor may contain a few thousand cells, including cancer cells. We define the average density/concentration (Ave) and total mass (TM) as follows

$$Ave = \frac{1}{R^3(t)}\int_0^{R(t)} X_i r^2 dr,\ TM = 4\pi\int_0^{R(t)} X_i r^2 dr.$$

Fig 2 shows the profiles of the average density of cells and concentration of proteins for the first 600 days, as the tumor radius $R(t)$ continues to grow, while Fig 3 shows the total mass of cells and proteins. Although the total mass of all the variables is growing continuously, the averages are not all monotone increasing. Cancer density dips for the first 80 days probably due to

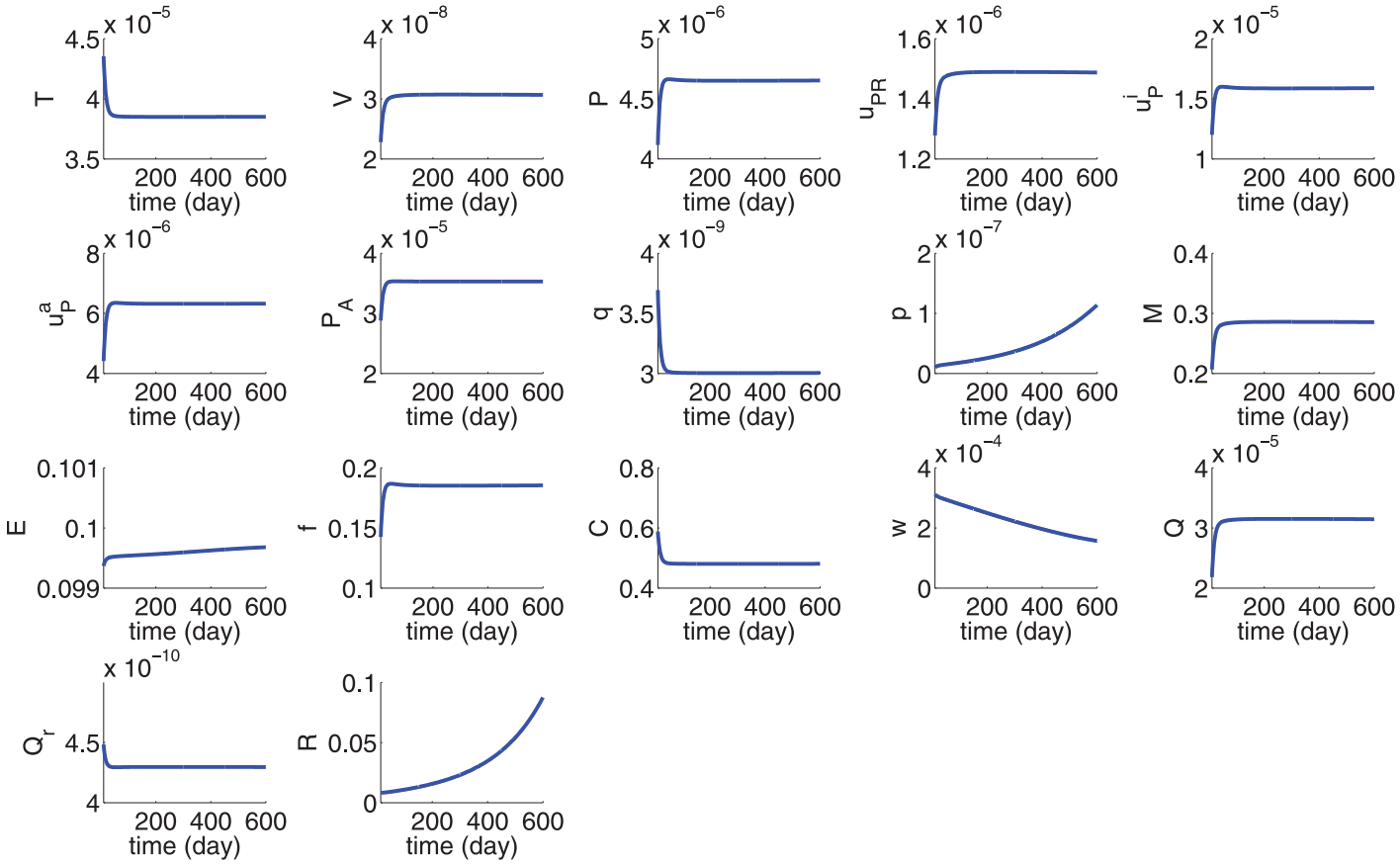

Fig 2. Average concentration of cytokines, average density of cells, and tumor radius $R(t)$ for the first 600 days with $R(0) = 10^{-2}$ cm = 100 μm. All the parameters are as in Tables 2 and 3.

doi:10.1371/journal.pone.0153508.g002

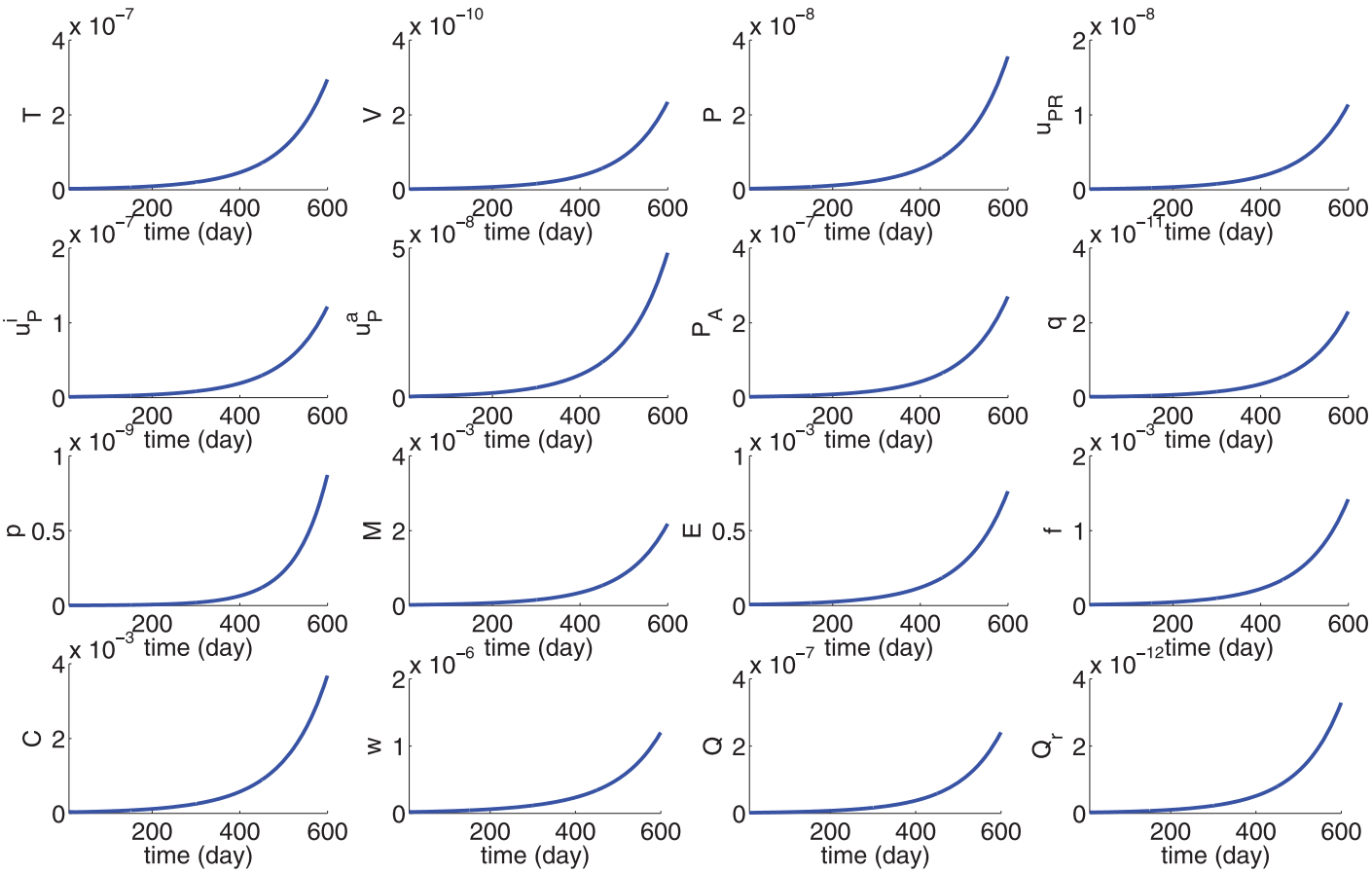

Fig 3. The total mass of cells and cytokines for the first 600 days with $R(0) = 10^{-2}$ cm = 100 μm. All the parameters are as in Tables 2 and 3.

doi:10.1371/journal.pone.0153508.g003

hypoxic conditions as the density of endothelial cells is still small (VEGF is still small). The average of oxygen is decreasing as cancer cells are increasing and consuming more oxygen, while the consumption of oxygen by macrophages, fibroblasts, and epithelial cells, combined, is also slightly increasing. uPA is growing after 80 days when fibroblast density begins to increase; PAI-1 mimics the profile of active uPA, while the concentrations of uPAR is relatively stable.

In estimating some of the parameters we assumed steady state of averages of densities of cells and concentrations of proteins, except for p and w. Fig 2 shows agreement with these assumed steady state averages. Thus the model simulations in Fig 2 are consistent with the assumptions made in the parameters estimation.

Harbeck et al. [20] measured the concentrations of uPA and PAI-1 in breast cancer survivors by the protein nanogram of protein antigen per milligram of tissue protein of breast tissue. They determined that when the risk of recurrence is high, PAI-1≈5×uPA. This proportion between PAI-1 and active uPA is seen also in Fig 2.

For the purpose of developing serum biomarkers we are interested in the total mass of uPAR in the growing tumor, rather than in the average density. Fig 3 shows that the total mass of cells and cytokines are increasing in time, but at different rates.

So far we have taken $R(0)$ fixed at $R_0 = 10^{-2}$ cm. We next want to use the model for diagnostic purposes. Our goal is to determine from one measurement of the total mass of uPAR at time t_0 after the primary breast cancer treatment the radius of the tumor at the same time t_0 and at any subsequent time t_1, $t_1 > t_0$. To do this we take $R_0 \in (10^{-2}, 5 \times 10^{-2})$ cm as a potential

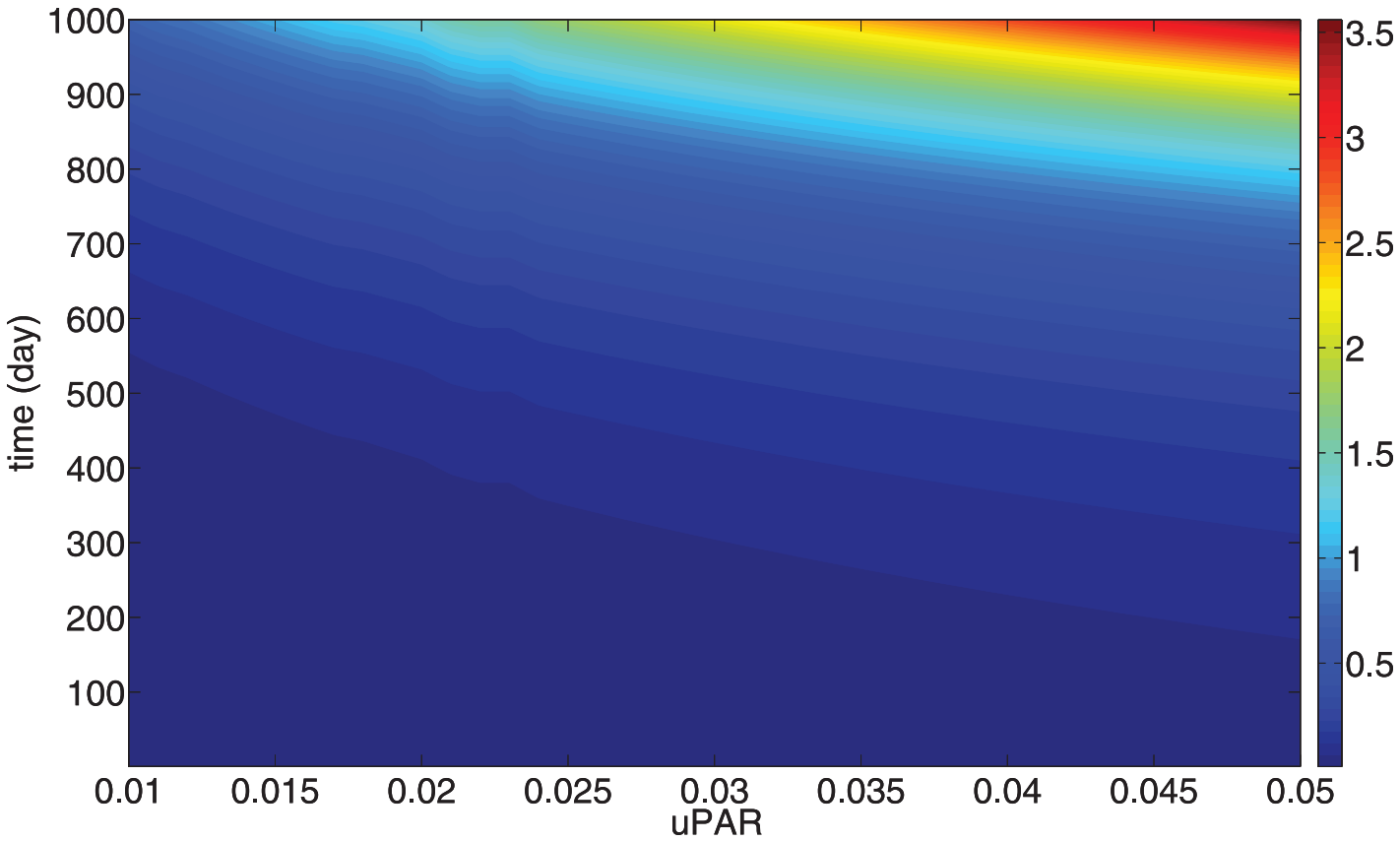

Fig 4. Color map for *R(t)*. R_0 ranges from 0.01 to 0.05 cm and t ranges from $t = 0$ to $t = 1000$ days. Color represents the size of the radius of the cancer. All the parameters are as in Tables 2 and 3.

doi:10.1371/journal.pone.0153508.g004

initial radius. For each R_0, we compute the tumor radius at time t, $R = R(R_0, t)$ and the total mass of uPAR at time t, uPAR(R_0, t).

Fig 4 shows R and Fig 5 shows the total mass of uPAR, at any (R_0, t) in the range $R_0 \in (10^{-2}, 5 \times 10^{-2})$ cm and $0 < t < 1000$ days. From these two figures we can generate a mapping from total uPAR(t) to R(t) which is independent of R_0, as follows: From a value of uPAR at some time t after primary breast cancer treatment, we estimate, by using Fig 4, the corresponding parameter R_0. We can then use Fig 5 to predict the value of R corresponding to this R_0 and the time t. The mapping is uPAR(t)→R(t) is shown in Fig 6, where the color bar determines the value of $R(t)$ for a given pair of uPAR and t.

The color map in Fig 6 is a prognostic map for recurrent breast cancer: when a patient's uPAR is measured t days after the primary breast cancer treatment, the color bar in Fig 6 predicts the size of the recurrent tumor.

Discussion

There are several mathematical models of breast cancer focusing on different aspects of the disease [28, 38, 56–58]. Our model is the first one to focus on biomarkers associated with the risk of breast cancer recurrence.

Cancer recurrence occurs in 10 to 20 percent of all breast cancer survivors. In order to avoid unnecessary radical treatment, it is important to diagnose a recurrent cancer as early as

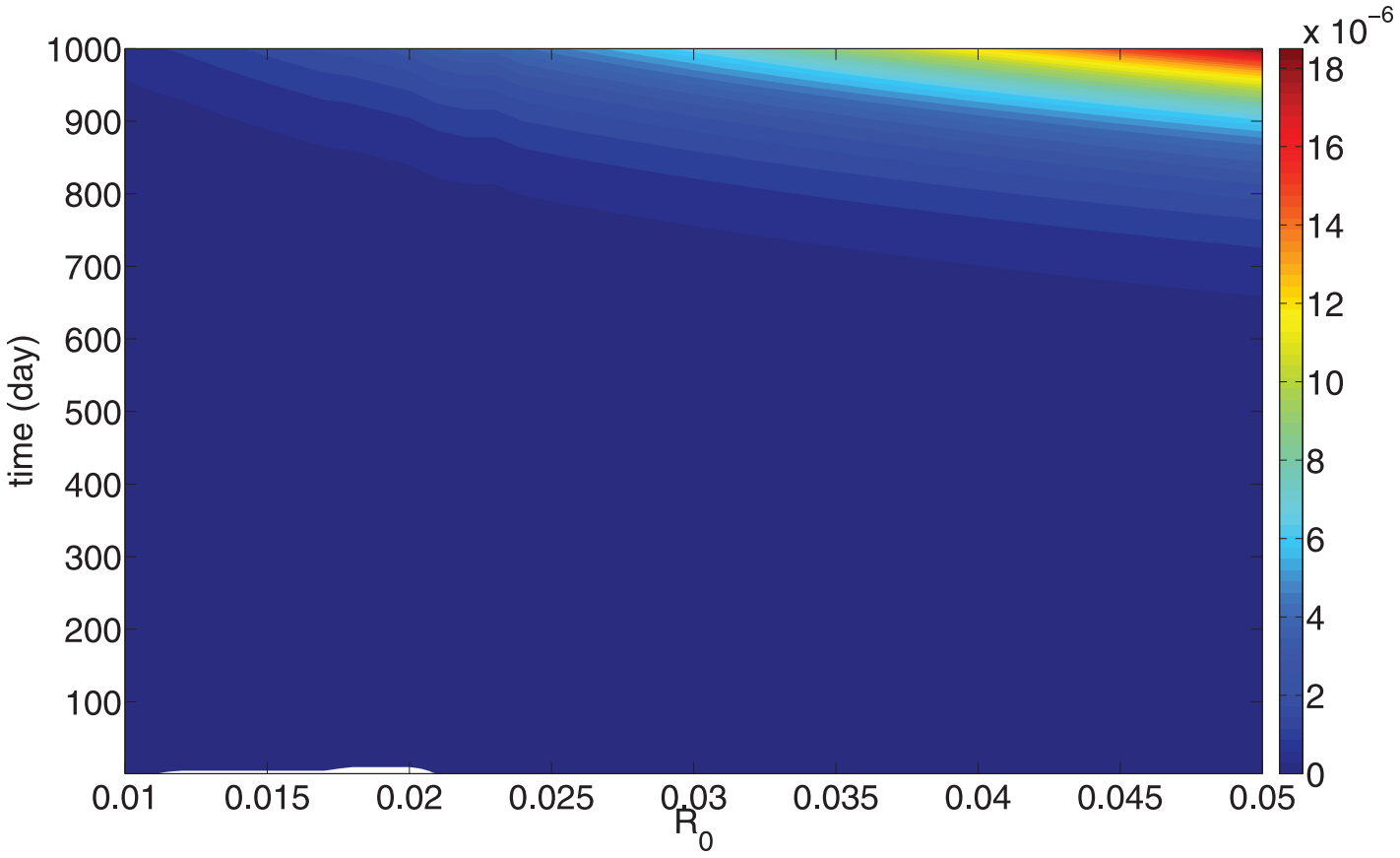

Fig 5. Color map for the total mass of uPAR. R_0 ranges from 0.01 to 0.05 cm and t ranges from $t = 0$ to $t = 1000$ days. Color represents the total mass of uPAR. All the parameters are as in Tables 2 and 3.

doi:10.1371/journal.pone.0153508.g005

possible. Although several tissue biomarkers have been identified, biopsy cannot be frequently repeated. This motivated the present study of focusing on potential serum biomarkers which are non-invasive. Of all the plasmiogen system tissue biomarkers only uPAR concentration significantly correlates with uPAR concentration in blood [22, 23]. For this reason we developed in this paper a mathematical model that quantifies the relation between tissue uPAR and the size of a recurrent cancer (Fig 6).

The mathematical model is represented by a system of partial differential equations in a growing tumor with radius $R(t)$. We assume a very small initial radius $R_0 \in (10^{-2}, 5 \times 10^{-2})$ cm, corresponding to cancer cells that survived after primary breast cancer treatment. The radius R_0 may vary from one patient to another. Nevertheless, Fig 6 shows that a patient's uPAR measured at any time within 1000 days after primary breast cancer treatment, can be used to estimate the cancer size (i.e., its radius) by the color bar. Furthermore, the initial R_0 can then be determined from Fig 4, and hence, by Fig 5 also the radius $R(t)$ for all subsequent times.

While the measurement of serum biomarkers for patient survival after primary breast cancer treatment is still being debated [8], we propose here uPAR as a potential serum biomarker. When clinical data become available to enable us to estimate the precise proportion of uPAR tissue concentration to plasma concentration, uPAR could then be used as plasma biomarker which informs the size of a recurrent tumor. The simulation results of Figs 4–6 can be extended to include smaller values of R_0, e.g. $0.005 \leq R_0 \leq 0.01$. For such values, it takes a significantly longer time for the tumor radius to reach a size that can be detected by self examination.

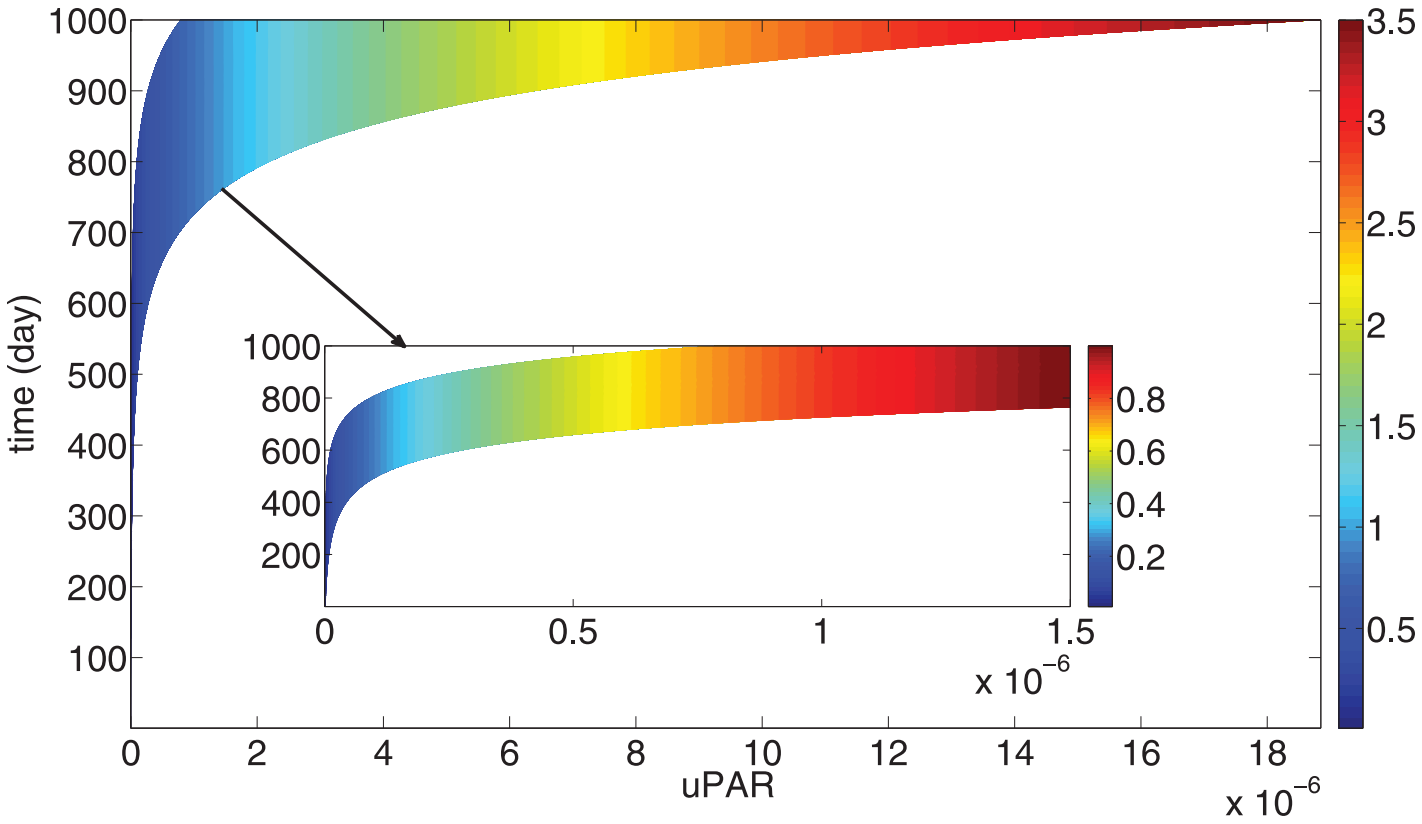

Fig 6. Color map for the total mass of uPAR(t) v.s. R(t). For any time t, $0 < t < 1000$ days, measurement uPAR in gm/cm^3 (on the horizontal axis) determines the size of the radius of the cancer in cm, using the column color. All the parameters are as in Tables 2 and 3.

doi:10.1371/journal.pone.0153508.g006

The simulation results rely heavily on parameters taken from the literature, sometimes in a different context, and on parameters estimated in this paper, sometimes rather crudely. For this reason we performed sensitivity analysis to determine how the radius of the tumor will vary when some of the parameters are increased or decreased.

In developing the mathematical model we made several simplifying assumptions: (i) the tumor is radially symmetric; (ii) the total density of cells at each point of the tissue is constant; and (iii) the cells are approximately of the same volume and surface area making the dispersion coefficient of cells equal. Furthermore, the mathematical model is minimal in the sense that includes just the plasminogen system (of uPA, uPAR, PAI-1), plasmin and MMP, tissue factor, VEGF, MCP-1, M-CSF, and the cells that produce these proteins or are activated by them, namely, macrophages, endothelial cells, fibroblasts and cancer cells. For these reasons, this work should be viewed as providing just a first step upon which a more elaborate and more comprehensive model could be developed in the future. When new data of uPAR expression level in patients of breast cancer recurrence become available, some of the parameters of the model will accordingly be adjusted to make the model simulations agree with patients data. Additional cytokines may then also be included, and the assumption of a spherical tumor may be changed to better reflects tumor histology.

Materials and Methods

All the parameters of the model are listed in Tables 2 and 3. Some of them are taken from the literature, while all the rest are estimated in this section.

Table 2. Parameters' description and value.

Parameter	Description	Value
D_T	diffusion coefficient of tissue factor	0.111 cm^2day^{-1} estimated
D_V	diffusion coefficient of VEGF	8.64×10^{-2} cm^2 day^{-1}[59]
D_P	diffusion coefficient of plasmin	0.212 cm^2day^{-1} estimated
$D_{u_{PR}}$	diffusion coefficient for uPAR	8.64×10^{-7} cm^2 day^{-1}[54]
D_{u_p}	diffusion coefficient of uPA	0.117 cm^2day^{-1} estimated
D_{P_A}	diffusion coefficient of PAI-1	0.127 cm^2day^{-1} estimated
D_q	diffusion coefficient of M-CSF	0.013 cm^2day^{-1}[54]
D_p	diffusion coefficient for MCP-1	1.29×10^{-2} cm^2 day^{-1}[54]
D_M	diffusion coefficient of macrophages	8.64×10^{-7} cm^2 day^{-1}[54]
D_E	diffusion coefficient for endothelial cells	8.64×10^{-7} cm^2 day^{-1}[54]
D_f	diffusion coefficient forfibroblasts	8.64×10^{-7} cm^2 day^{-1}[54]
D_C	diffusion coefficient for cancer cells	8.64×10^{-7} cm^2 day^{-1}[54]
D_w	diffusion coefficient for oxygen	4.32×10^{-2} cm^2 day^{-1}[54]
D_Q	diffusion coefficient of MMP	4.32×10^{-2} cm^2 day^{-1}[54]
$D_{Q,}$	diffusion coefficient for TIMP	4.32×10^{-2} cm^2 day^{-1}[54]
A_T	production rate of tissue factor	3.23×10^{-5} g/ml/day estimated
λ_{TC}	production rate of tissue factor by cancer cell	5.7×10^{-5} day^{-1} estimated
λ_{VC}	production rate of VEGF by cancer cell	2×10^{-8} *g/ml*/day estimated
λ_{VT}	production rate of VEGF by TF	2 estimated
λ_{VM}	production rate of VEGF by macrophages	2×10^{-6} *g/ml*/day estimated
λ_P	activation rate of plasmin	2.42×10^{-6} g/ml/day estimated
λ_{Pu}	activation rate of plasmin by uPA	10.5 estimated
$\lambda_{u_{PR}\,M}$	production rate of uPAR by macrophages	6.21×10^{-6} day^{-1} estimated
$\lambda_{u_{PR}\,C}$	production rate of uPAR by cancer	1.242×10^{-6} day^{-1} estimated
λ_{uf}	production rate of uPA by fibroblasts	2.057×10^{-4} day^{-1} estimated
λ_u	production rate of uPA	1.92 day^{-1} estimated
λ_{PC}	activation rate of PAI-1 by cancer cells	8×10^{-5} day^{-1} estimated
λ_{Pf}	activation rate of PAI-1 by fibroblasts	8.4×10^{-4} day^{-1} estimated
λ_{PM}	activation rate of PAI-1 by macrophages	4×10^{-4} day^{-1} estimated
λ_{qC}	production rate of GM-CSF by cancer cell	3×10^{-8} day^{-1}[38]
λ_p	production rate of MCP-1 by macrophages	1.9×10^{-6} day^{-1}[38]
λ_E	production rate of endothelial cells	0.7 day^{-1}[31]
A_f	based production rate of fibroblasts	10^{-3} *g/ml*/day [40]
λ_{fC}	production rate of fibroblasts	5×10^{-3} day^{-1} estimated
β	flux rate of monocytes	0.3 day^{-1} estimated
λ_{Cf}	production rate of cancer cells	0.06 day^{-1} estimated
λ_{Cu_P}	production rate of cancer cell by uPA	0.05 day^{-1} estimated
λ_{wC}	production rate of cancer by oxygen	0.6 g/cm^{3}day^{-1} estimated
λ_w	production rate of oxygen by endothelial cells	7×10^{-2}[31, 38]
λ_{QM}	production rate of MMP by macrophages	3×10^{-4} day^{-1}[40]
λ_{QP}	production rate of MMP by plasmin	2 estimated
$\lambda_{Q,\,M}$	production rate of TIMP by macrophages	6×10^{-5} day^{-1}[40]
λ_{pf}	activation rate of ECM by fibroblasts	3×10^{-3} day^{-1}[40]

doi:10.1371/journal.pone.0153508.t002

Table 3. Parameters' description and value.

Parameter	Description	Value
d_T	degradation rate oftissue factor	1.85 day^{-1}[64]
d_V	degradation rate of VEGF	12.6 day^{-1}[31]
d_P	degradation rate of plasmin	1.39 day^{-1}[67]
$d_{u_{PR}}$	degradation rate of uPAR	1.38 day^{-1}[76, 77]
$d_{u_P^a}$	degradation rate of active uPA	3.2 day^{-1}[76, 77]
$d_{u_P^i}$	degradation rate of inactive uPA	2.4 day^{-1}[76, 77]
d_{P_A}	degradation rate of PAI-1	8.32 day^{-1}[80]
d_q	degradation rate of GM-CSF	4.8 day^{-1}[38]
d_p	degradation rate of MCP-1	1.73 day^{-1}[31, 54]
d_M	death rate of macrophages	0.015 day^{-1}[54]
d_E	degradation rate of endothelial cells	0.69 day^{-1}[54]
d_f	death rate of fibroblasts	1.66×10^{-2} day^{-1}[40]
d_C	death rate of cancer cells	0.5 day^{-1}[31]
d_{wM}	consumption rate of oxygen by macrophages	80 *ml*/*g*/day [31]
d_{wC}	consumption rate of oxygen by cancer cells	40 *ml*/*g*/day [31]
d_{wf}	consumption rate of oxygen by fibroblasts	80 *ml*/*g*/day estimated
d_{QQ_r}	binding rate of MMP to TIMP	4.98×10^8 cm^3 g^{-1} day^{-1}[40, 54]
d_Q	degradation rate of MMP	4.32 day^{-1}[40, 54]
$d_{Q,Q}$	binding rate of TIMP to MMP	1.04×10^9 cm^3 g^{-1} day^{-1}[40, 54]
d_{Q_r}	degradation rate of TIMP	21.6 day^{-1}[40, 54]
d_ρ	based degradation rate of ECM	0.37 day^{-1}[40, 54]
$d_{\rho Q}$	degradation rate of ECM by MMP	2.59×10^7 cm^3 g^{-1} day^{-1}[40, 54]
K_T	TF half-saturation	10^{-4} gcm^{-3} estimated
K_{P_A}	PAI-1 half-saturation	4.19×10^{-6} g/ml estimated
$K_{u_{PR}}$	uPAR half-saturation	1.8×10^{-6} g/ml estimated
K_p	MCP-1 half-saturation	2×10^{-7} g/ml estimated
K_E	carrying capacity of endothelial cells	5×10^{-3} gcm^{-3}[31]
K_C	cancer cells half-saturation	0.5 gcm^{-3} estimated
K_f	fibroblast half-saturation	0.1 gcm^{-3} estimated
K_P	plasmin half-saturation	4.4×10^{-6} g/ml estimated
K_V	VEGF half-saturation	7×10^{-8} g/ml estimated
M_0	monocytes density in the blood	5×10^{-5} g/ml [54]
V_0	threshold VEGF concentration	3.65×10^{-10} gcm^{-3}[31]
C_0	carrying capacity of cancer cells	0.75 gcm^{-3}[31]
q_0	GM-CSF half saturation	10^{-9} gcm^{-3}[38]
w_0	oxygen saturation	4.65×10^{-4} g/ml [31]
E_0	endothelial cells density at tumor microenviroment	2.5×10^{-3} g/ml [31]
ρ_0	ECM saturation	10^{-3} g/ml [54]
χ_C	chemotactic coefficient	10 [54]
w_h	oxygen half-saturation	10^{-4} gcm^{-3}[31]
$\widetilde{\alpha_w}$	influx rae for oxygen	1 estimated
$\widetilde{\alpha_E}$	influx rate for endothelial cells	1 estimated

doi:10.1371/journal.pone.0153508.t003

Diffusion coefficients

The diffusion coefficients of proteins (Y) are proportional to the molecular surface area [54], which is proportional to $M_Y^{2/3}$, where M_Y is the molecular weight [54]. Accordingly, we can have the following relation:

$$D_Y = \frac{M_Y^{2/3}}{M_V^{2/3}} D_V,$$

where M_V and D_V are the molecular weight and diffusion coefficient of VEGF. Since $D_V = 8.64 \times 10^{-2}\ cm^2\ \text{day}^{-1}$[59], $M_V = 24$ kDa [60] and $M_P = 92$ kDa [61], $M_{u_P} = 38$ kDa [56], $M_T = 35$ kDa [62] and $M_{P_A} = 43$ kDa [63], we get $D_P = 0.212\ cm^2\text{day}^{-1}$, $D_{u_P} = 0.117\ cm^2\text{day}^{-1}$, $D_T = 0.111\ cm^2\text{day}^{-1}$ and $D_{P_A} = 0.127\ cm^2\text{day}^{-1}$.

Eq (1)

- d_T: The tissue factor half life is 9 hours [64], hence $d_T = 1.85\ \text{day}^{-1}$.
- A_T: The concentration of tissue factor in cancer is 3.5×10^{-5} g/ml [65]. The ratio of tissue factor in healthy to disease in plasma is 1:2 [66]. We assume larger ratio in breast tissue, so that in the healthy case $T = 2 \times 10^{-4}$ g/ml and take $K_T = 10^{-4}$ g/ml. From Eq (1), in steady state for the healthy case, we get $A_T = d_T\, T = 3.23 \times 10^{-5}$ g/ml/day.
- λ_{TC}: We assume that most of the tumor is populated with cancer cells, and take $C = 0.5$ g/ml. As in the deviation of Eq (12), to simplify the model and to estimate some of the parameters, we assume that cytokine equations are in steady-state. From the steady-state of Eq (1) in disease state we have $A_T + \lambda_C\, C = d_T \times 3.5 \times 10^{-5}$, so that $\lambda_{TC} = 5.7 \times 10^{-5}\ \text{day}^{-1}$.

Eq (2)

According to (31, 39) λ_{VC} varies in the range of 10^{-21} to 10^{-20} in units of g/s/cell, and the production of VEGF by tumor associated macrophages is far larger than the production of VEGF by cancer cells. Accordingly we take $\lambda_{VC} = 2 \times 10^{-8}$/day and $\lambda_{VM} = 2 \times 10^{-6}$/day. We also assume that T enhances cancer-cells production by less than 200% and take $\lambda_{VT} = 2$.

Eq (3)

- d_P: The half life of plasmin is 0.5 day [67], hence $d_P = 1.39$/day.
- λ_{Pu}: uPAR in disease is 3/2 uPAR in healthy case [68]. Plasminogen binding to cancer cells was increased by 3/2 in disease compared to the healthy [69]. Hence we assume that

$$\lambda_{Pu} \frac{u_P^a}{K_{P_A} + P_A} = \frac{3}{2},$$

where $P_A = 8.39 \times 10^{-6}$[70], and $u_P^a = 1.8 \times 10^{-6}$ g/ml [70, 71]. By taking $K_{P_A} = \frac{1}{2} P_A = 4.19 \times 10^{-6}$, we get $\lambda_{Pu} = 10.5$.

- λ_P: The molecular weight of plasminogen is 92 kDa [61] while molecular weight of uPA is 38 kDa [56]. The concentration of uPA in breast cancer is 1.8×10^{-6} g/ml [70, 71]. We assume that the number of uPA proteins in plasma is the same as the number of plasmin proteins, so

that

$$\frac{\text{the concentration of plasmin}}{\text{the concentration of uPA}} = \frac{92 \text{ kDa}}{38 \text{ kDa}}.$$

Therefore, the concentration of plasmin in breast cancer is approximately 4.4×10^{-6} g/ml. By Eq (3), we have

$$\lambda_p(1 + 3/2) = d_p P,$$

which implies $\lambda_P = 2.42 \times 10^{-6}$ g/ml/day.

Eq (4)

- $d_{u_{PR}}$: The half life of uPAR is 12 hours [72], therefore $d_{u_{PR}} = 1.38$/day.
- $\lambda_{u_{PR}M}$ and $\lambda_{u_{PR}C}$: The concentration of uPAR in breast cancer is 1.8×10^{-6} g/ml [70, 71]. The concentration of uPAR in normal healthy breast is significantly smaller [73]; we take it to be approximately 10 times smaller. In healthy case, $M = 0.04$ g/ml [74], and from

$$\lambda_{u_{PR}M} M - d_{u_{PR}} u_{PR} = 0$$

we get, $\lambda_{u_{PR}M} = 6.21 \times 10^{-6}$ day^{-1}.
In disease case, $M = 0.3$ g/ml [75]. Taking $C = 0.5$ g/ml in the steady state equation

$$\lambda_{u_{PR}M} M + \lambda_{u_{PR}C} C - d_{u_{PR}} u_{PR} = 0,$$

we get $\lambda_{u_{PR}C} = 1.242 \times 10^{-6}$ day^{-1}.

Eqs (5) and (6)

- $d_{u_P^i}$ and $d_{u_P^a}$: The half life of activated uPA is 5 hours [76, 77], therefore $d_{u_P^a} = 3.2$/day. We assume that inactivated uPA degrades slower, and take $d_{u_P^i} = 2.4$/day.
- λ_{uf}: The concentration of uPA in normal healthy tissue is estimated to $u_P^i = 6 \times 10^{-6}$ g/ml [78], and fibroblast density is 0.07 g/ml [40]. From

$$\lambda_{uf} f - d_{u_p^i} u_P^i = 0$$

we get $\lambda_{uf} = 2.057 \times 10^{-4}$ day^{-1}.

- λ_u: We use the steady state equation

$$\lambda_u u_P^i \frac{u_{PR}}{K_{u_{PR}} + u_{PR}} - d_{u_p^a} u_P^a = 0$$

where we take $K_{u_{PR}} = u_{PR} = 1.8 \times 10^{-6}$ g/ml, and $u_p^a = 1.8 \times 10^{-6}$ g/ml [70, 71]. Since $u_P^i / u_P^a = 3.3$, we get $\lambda_u = 1.92$ day^{-1}.

Eq (7)

The PAI-1 concentration in breast cancer is 12 ng/mg [70] (and $\frac{\text{mg protein}}{\text{mg}} = 1.43$ [79]), which implies that $P_A = 12 \times 10^{-9}/1.43/10^{-3} = 8.39 \times 10^{-6}$ g/ml. Since $d_{P_A} = 8.32$ day^{-1}[80], we have

$d_{P_A} P_A = 7 \times 10^{-5}$ g/ml/day. In the steady state, we have

$$\lambda_{PC} C + \lambda_{Pf} f + \lambda_{PM} M = d_{P_A} P_A = 7 \times 10^{-5} g/ml/\text{day}.$$

However, since the tumor is growing, the left-hand side should be larger than 7×10^{-5}. We take the left-hand side to be 4 times larger than 7×10^{-5}. We also assume that the first term $\lambda_{PC} C$ contributes $\frac{1}{7}$-th, and that, the remaining two terms contribute each $\frac{3}{7}$-th of the total 7×10^{-5}. From $\lambda_{PC} C = 4 \times 10^{-5}$ g/ml/day, where $C = 0.5$ g/ml, we get $\lambda_{PC} = 8 \times 10^{-5}$/day. Similarly, from $\lambda_{Pf} f = \lambda_{PM} M = 1.2 \times 10^{-4}$ g/ml/day and $f = 0.14$ g/ml, $M = 0.3$ g/ml, we get $\lambda_{Pf} = 8.4 \times 10^{-4}$/day and $\lambda_{PM} = 4 \times 10^{-4}$/day.

Eq (10)

From steady state of Eq (9) with $M = 0.3\ g/cm^3$, $\lambda_p(w) \sim \lambda_p$, $d_p = 1.73$/day and $q/(q_0 + q) \sim 1/2$, we take an approximate steady state of p to be $2 \times 10^{-7}\ g/cm^3$, and $K_p = 2 \times 10^{-7}\ g/cm^3$. The parameter β is unknown; in [40] it was chosen to be 0.2/day; here we take it to be 0.3/day.

Eq (12)

In Eq (12) production term $\lambda_{fC} f \frac{C}{K_C + C}$ is due to cytokines secreted by cancer cells. We assume that this term is only a fraction of the death rate $d_f f$ of fibroblasts, where $d_f = 16.6 \times 10^{-3}$/day, and take $\lambda_{fC} = 5 \times 10^{-3}$/day.

Eq (13)

$\lambda_C(w)$ accounts for the proliferation rate minus the death rate by necrosis, while d_C is the death rate by apoptosis. In transgenic mice $\lambda_C(w)$ is large [31, 38], and cancer develops within a few days. Since breast tumor in human develops much slower, on the time scale of years, we take $\lambda_C(w) = 0.6 \frac{w}{w_h}$ day^{-1} if $w < w_h$ and $\lambda_C(w) = 0.6$ day^{-1} if $w > w_h$, while $d_C = 0.5$ day^{-1}[31]. We assume that the enhanced proliferation rate by fibroblast and by u_p^a binding to u_{PR} are small, and take $\lambda_{Cf} = 0.06$ day^{-1} and $\lambda_{Cup} = 0.05$ day^{-1}.

In steady healthy state, we have by Eq (12), $A_f = d_f f$ where $A_f = 10^{-3}\ g/cm^3$/day, $d_f = 1.66 \times 10^{-2}$/day. So $f = 6.02 \times 10^{-2}\ g/cm^3$. Accordingly, we take the half-saturation $K_f = 0.1\ g/cm^3$

Eq (14)

We assume that fibroblasts consume oxygen at the same rate as macrophages, so that $d_{wf} = d_{wM} = 80\ cm^3/g$/day by [31].

Eq (15)

From the steady state of Eq (3), with no activated uPA, we get $P = \frac{\lambda_P}{d_P}$. Since $d_P = 1.39$/day [67] and λ_P was estimated (in Eq (3)) by $2.42 \times 10^{-6}\ g/cm^3$/day, we get $P = 1.74 \times 10^{-6}\ g/cm^3$. With active uPA in Eq (3), this value of P should be increased by the factor $1 + \lambda_{P_u} \frac{u_P^a}{K_{P_A} + P_A}$, so accordingly we take the half-saturation K_P to be $4.4 \times 10^{-6}\ g/cm^3$.

Boundary conditions

Since most VEGF is produced by tumor associated macrophages [31, 39]. the steady state of Eq (2) yields

$$(1 + \varepsilon)\lambda_{VM} M = d_V V$$

where $\varepsilon < 1$, $d_V = 12.6$/day [31] and $\lambda_{VM} = 2 \times 10^{-6}$/day. Taking $M = 0.3$ g/ml and $\varepsilon = 1/2$, we get the approximate value $V = 7 \times 10^{-8}$ g/ml. We accordingly take $K_V = 7 \times 10^{-8}$. We also take $\widetilde{\alpha_w}$ and $\widetilde{\alpha_E}$ to be of order 1, and for simplicity choose $\widetilde{\alpha_w} = \widetilde{\alpha_E} = 1$; however, other choices affect the model simulations only very little (not shown here).

Sensitivity analysis

We performed sensitivity analysis on the all production parameters of the system (1)-(17). Following the method in [81], we performed Latin hypercube sampling and generated 1000 samples to calculate the partial rank correlation (PRCC) and the p-values with respect to the radius of the tumor at day 600. The results are shown in Fig 7 (The p-value was <0.01).

The most positively correlated production parameters are λ_{VM} (the production of VEGF by macrophages), λ_u (the production uPA activator), λ_{Cf} (λ_{Cf} and λ_{fC} represent the cross-talk between cancer cells and fibroblasts, which increases the number of cancer cells). The most negatively correlated production parameters are λ_{Pf} and λ_{PC} (which increase, together with λ_{PM}, the production of PAI-1, thus increasing the blockage on uPA and the consequently proliferation of cancer cells), and λ_P (which increases plasmin, and hence also PAI-1).

The remaining parameters are mildly correlated to tumor growth, and their correlation (+ or -) is agreement with the model description in Fig 1.

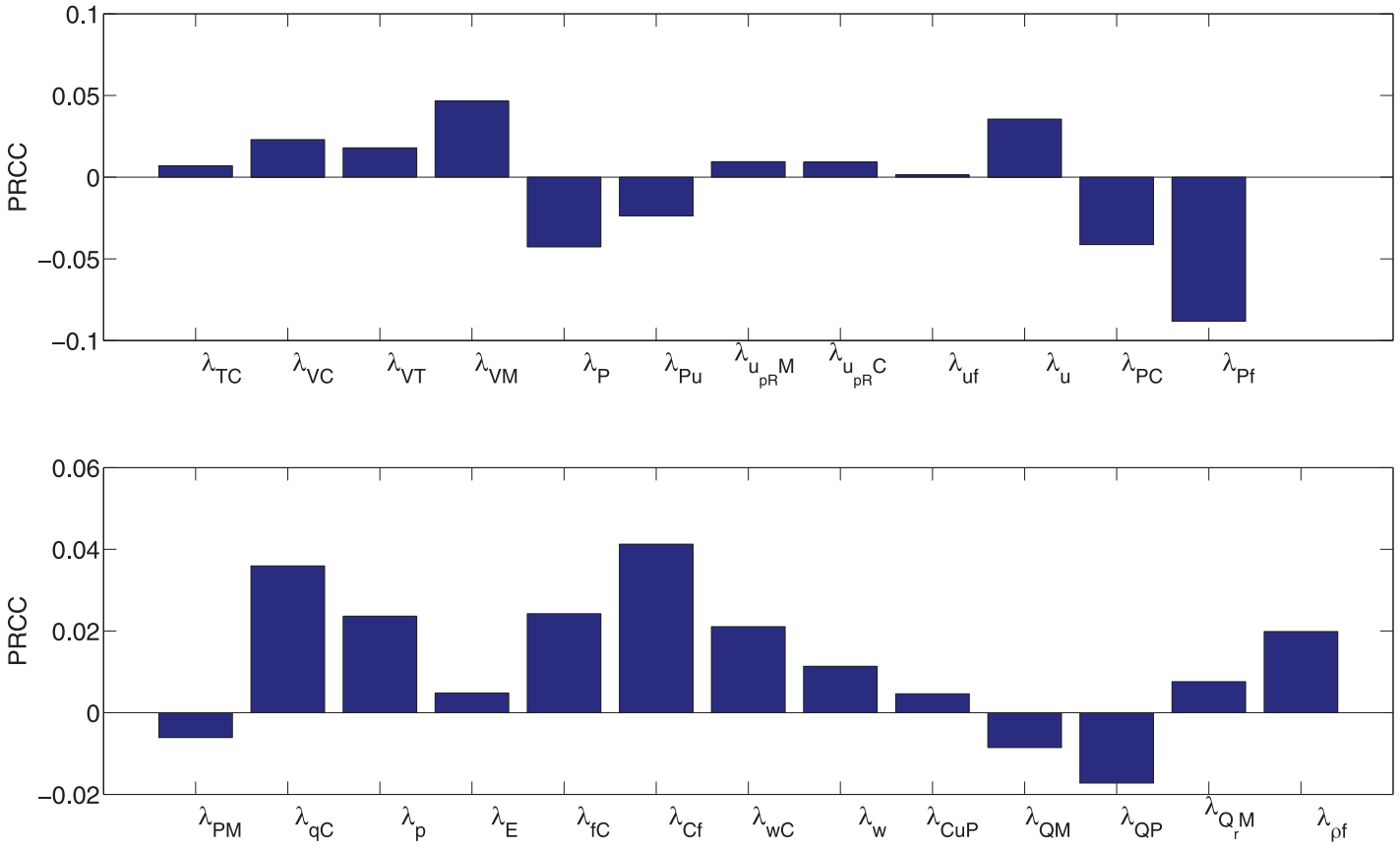

Fig 7. The sensitivity analysis for the cytokine production rates. The figure shows the partial rank correlation (PRCC) between the cytokine production rate and the radius of tumor. All the parameters are as in Tables 2 and 3.

doi:10.1371/journal.pone.0153508.g007

Computational Method

In order to illustrate our numerical method, we consider the following convection-diffusion equation:

$$\frac{\partial X}{\partial t} + div(vX) = D\nabla^2 X + F_X, \tag{22}$$

where F_X accounts for all the 'active' terms. Since the model we consider is a free boundary problem, we employ the moving mesh method to compute it. We write Eq (33) can be written in the total derivative form

$$\frac{dX(r(t),t)}{dt} + div(v)X = D\nabla^2 X(r(t),t) + F_X.$$

Let r_i^n, X_i^n denote numerical approximations of i-th grid point and $X(r_i^n, t)$, respectively, when $t = n\tau$, where τ is the time stepsize. The discretization is derived by the explicit Euler finite difference scheme, i.e.,

$$\frac{X_i^{n+1} - X_i^n}{\tau} + \left(\frac{v_r}{r_i^n} + v_i^n\right)X_i^n = D\left(X_{rr} + \frac{X_r}{r_i^n}\right) + F_X,$$

where $X_r = \frac{h_{-1}^2 X_{i+1}^n - h_1^2 X_{i-1}^n - (h_1^2 - h_{-1}^2)X_i^n}{h_1(h_{-1}^2 - h_1 h_{-1})}$, $X_{rr} = 2\frac{h_{-1}X_{i+1}^n - h_1 X_{i-1}^n + (h_1 - h_{-1})X_i^n}{h_1(h_1 h_{-1} - h_{-1}^2)}$, and $h_{-1} = r_{i-1}^n - r_i^n$, $h_1 = r_{i+1}^n - r_i^n$. Then the mesh is moving by $r_i^{n+1} = r_i^n + v_i^n\tau$, where v_i^n is solved by the velocity equation. In order to make the Euler method stable, we take $\tau \leq \frac{min\{h_1, h_{-1}\}}{2D}$.

Acknowledgments

The authors have been supported by the Mathematical Biosciences Institute and the National Science Foundation under Grant DMS 0931642. The authors thank J.F. Rabajante for this many comments that helped improve the presentation of the paper.

Author Contributions

Analyzed the data: WH AF. Contributed reagents/materials/analysis tools: WH AF. Wrote the paper: WH AF.

References

1. Foundation BCR. Breast cancer statistics & resources. 2016.
2. Foundation USBCR. U.S. Breast cancer statistics. 2016.
3. Dos Anjos Pultz B, da Luz FA, de Faria PR, Oliveira AP, de Araujo RA, Silva MJ. Far beyond the usual biomarkers in breast cancer: a review. J Cancer. 2014; 5(7):559–571. doi: 10.7150/jca.8925 PMID: 25057307
4. Kantelhardt EJ, Vetter M, Schmidt M, Veyret C, Augustin D, et al. Prospective evaluation of prognostic factors uPA/PAI-1 in node-negative breast cancer: phase III NNBC3-Europe trial (AGO, GBG, EORTC-PBG) comparing FEC versus FECDocetaxel. BMC Cancer. 2011; 11:140. doi: 10.1186/1471-2407-11-140 PMID: 21496284
5. Rubinstein WS, O'Neill SM, Peters JA, Rittmeyer LJ, Stadler MP. Mathematical modeling for breast cancer risk assessment. State of the art and role in medicine. Oncology (Williston Park, NY). 2002; 16 (8):1082–1094.
6. Chung L, Moore K, Phillips L, Boyle FM, Marsh DJ, Baxter RC. Novel serum protein biomarker panel revealed by mass spectrometry and its prognostic value in breast cancer. Breast Cancer Res. 2014; 16 (3):R63. doi: 10.1186/bcr3676 PMID: 24935269

7. Jesneck JL, Mukherjee S, Yurkovetsky Z, Clyde M, Marks JR, Lokshin AE, et al. Do serum biomarkers really measure breast cancer? BMC Cancer. 2009; 9:164. doi: 10.1186/1471-2407-9-164 PMID: 19476629
8. Mirabelli P, Incoronato M. Usefulness of traditional serum biomarkers for management of breast cancer patients. Biomed Res Int. 2013; 2013:685641. doi: 10.1155/2013/685641 PMID: 24350285
9. Dublin E, Hanby A, Patel NK, Liebman R, Barnes D. Immunohistochemical expression of uPA, uPAR, and PAI-1 in breast carcinoma. Fibroblastic expression has strong associations with tumor pathology. Am J Pathol. 2000; 157(4):1219–1227. doi: 10.1016/S0002-9440(10)64637-8 PMID: 11021826
10. Mego M, Karaba M, Minarik G, Benca J, Sedlackova T, et al. Relationship between circulating tumor cells, blood coagulation, and urokinase-plasminogen-activator system in early breast cancer patients. Breast J. 2015; 21(2):155–160. doi: 10.1111/tbj.12388 PMID: 25623304
11. Nielsen BS, Sehested M, Duun S, Rank F, Timshel S. Urokinase plasminogen activator is localized in stromal cells in ductal breast cancer. Lab Invest. 2001; 81(11):1485–1501. doi: 10.1038/labinvest.3780363 PMID: 11706057
12. Didiasova M, Wujak L, Wygrecka M, Zakrzewicz D. From plasminogen to plasmin: role of plasminogen receptors in human cancer. Int J Mol Sci. 2014; 15(11):21229–21252. doi: 10.3390/ijms151121229 PMID: 25407528
13. Duffy M, McGowan P, Harbeck N, Thomssen C, Schmitt M. uPA and PAI-1 in breast cancer: validated for clinical use in level-of-evidence-1 studies. Breast Cancer. 2014; 16:428. doi: 10.1186/s13058-014-0428-4
14. Gandhari M, Arens N, Majety M, Dorn-Beineke A, Hildenbrand R. Urokinase-type plasminogen activator induces proliferation in breast cancer cells. Int J Oncol. 2006; 28(6):1463–1470. PMID: 16685447
15. H KC, B M. The role of plasminogen-plasmin system in cancer. Coagulation in Cancer. 2009; 4:43–65.
16. Hildenbrand R, Gandhari M, Stroebel P, Marx A, Allgayer H, Arens N. The urokinase-system—role of cell proliferation and apoptosis. Histol Histopathol. 2008; 23(2):227–236. PMID: 17999379
17. Li WY, Chong SS, Huang EY, Tuan TL. Plasminogen activator/plasmin system: a major player in wound healing? Wound Repair Regen. 2003; 11(4):239–247. doi: 10.1046/j.1524-475X.2003.11402.x PMID: 12846910
18. Ruf W, Yokota N, Schaffner F. Tissue factor in cancer progression and angiogenesis. Thromb Res. 2010; 125 Suppl 2:S36–38. doi: 10.1016/S0049-3848(10)70010-4 PMID: 20434002
19. Harbeck N, Dettmar P, Thomssen C, Berger U, Ulm K, Kates R, et al. Risk-group discrimination in node-negative breast cancer using invasion and proliferation markers: 6-year median follow-up. Br J Cancer. 1999; 80(3-4):419–426. doi: 10.1038/sj.bjc.6690373 PMID: 10408848
20. Harbeck N, Schmitt M, Vetter M, Krol J, Paepke D, et al. Prospective Biomarker Trials Chemo N0 and NNBC-3 Europe Validate the Clinical Utility of Invasion Markers uPA and PAI-1 in Node-Negative Breast Cancer. Breast Care (Basel). 2008; 3(s2):11–15.
21. Harris L, Fritsche H, Mennel R, Norton L, Ravdin P, et al. American Society of Clinical Oncology 2007 update of recommendations for the use of tumor markers in breast cancer. J Clin Oncol. 2007; 25 (33):5287–5312. doi: 10.1200/JCO.2007.14.2364 PMID: 17954709
22. Rha SY, Yang WI, Gong SJ, Kim JJ, Yoo NC, Roh JK, et al. Correlation of tissue and blood plasminogen activation system in breast cancer. Cancer Lett. 2000; 150(2):137–145. doi: 10.1016/S0304-3835(99)00376-6 PMID: 10704735
23. Guney N, Soydine HO, Derin D, Tas F, Camlica H, Duranyildiz D, et al. Serum and urine survivin levels in breast cancer. Med Oncol. 2006; 23(3):335–339. doi: 10.1385/MO:23:3:335 PMID: 17018890
24. Memarzadeh S, Kozak KR, Chang L, Natarajan S, Shintaku P, Reddy ST, et al. Urokinase plasminogen activator receptor: Prognostic biomarker for endometrial cancer. Proc Natl Acad Sci USA. 2002; 99 (16):10647–10652. doi: 10.1073/pnas.152127499 PMID: 12130664
25. Delozier T, Switsers O, Genot JY, Ollivier JM, Hery M. Delayed adjuvant tamoxifen: ten-year results of a collaborative randomized controlled trial in early breast cancer (TAM-02 trial). Ann Oncol. 2000; 11 (5):515–519. doi: 10.1023/A:1008321415065 PMID: 10907942
26. Romero L, Klein L, Ye W, Holmes D, Soni R, Silberman H, et al. Outcome after invasive recurrence in patients with ductal carcinoma in situ of the breast. Am J Surg. 2004; 188(4):371–376. doi: 10.1016/j.amjsurg.2004.06.034 PMID: 15474428
27. Freedman GM, Fowble BL. Local recurrence after mastectomy or breast-conserving surgery and radiation. Oncology (Williston Park, NY). 2000; 14(11):1561–1581.
28. Bluff JE, Brown NJ, Reed MW, Staton CA. Tissue factor, angiogenesis and tumour progression. Breast Cancer Res. 2008; 10(2):204. doi: 10.1186/bcr1871 PMID: 18373885

29. Zhang X, Yu H, Lou JR, Zheng J, Zhu H. MicroRNA-19 (miR-19) regulates tissue factor expression in breast cancer cells. J Biol Chem. 2011; 286(2):1429–1435. doi: 10.1074/jbc.M110.146530 PMID: 21059650

30. Eubank TD, Roberts RD, Khan M, Curry JM, Nuovo GJ. Granulocyte macrophage colony-stimulating factor inhibits breast cancer growth and metastasis by invoking an anti-angiogenic program in tumor-educated macrophages. Cancer Res. 2009; 69(5):2133–2140. doi: 10.1158/0008-5472.CAN-08-1405 PMID: 19223554

31. Szomolay B, Eubank T, Roberts RD, Marsh CB, Friedman A. Modeling the inhibition of breast cancer growth by GM-CSF. J Theor Biol. 2012; 303:141–151. doi: 10.1016/j.jtbi.2012.03.024 PMID: 22763136

32. Mantovani A, Schioppa T, Porta C, Allavena P, Sica A. Role of tumor-associated macrophages in tumor progression and invasion. Cancer Metastasis Rev. 2006; 25(3):315–322. doi: 10.1007/s10555-006-9001-7 PMID: 16967326

33. Hildenbrand R, Wolf G, Bohme B, Bleyl U, Steinborn A. Urokinase plasminogen activator receptor (CD87) expression of tumor-associated macrophages in ductal carcinoma in situ, breast cancer, and resident macrophages of normal breast tissue. J Leukoc Biol. 1999; 66(1):40–49. PMID: 10410988

34. LeBeau AM, Duriseti S, Murphy ST, Pepin F, Hann B. Targeting uPAR with antagonistic recombinant human antibodies in aggressive breast cancer. Cancer Res. 2013; 73(7):2070–2081. doi: 10.1158/0008-5472.CAN-12-3526 PMID: 23400595

35. Sieuwerts AM, Klijn JG, Henzen-Logmand SC, Bouwman I, Van Roozendaal KE, Peters HA, et al. Urokinase-type-plasminogen-activator (uPA) production by human breast (myo) fibroblasts in vitro: influence of transforming growth factor-beta(1) (TGF beta(1)) compared with factor(s) released by human epithelial-carcinoma cells. Int J Cancer. 1998; 76(6):829–835. doi: 10.1002/(SICI)1097-0215(19980610)76:6%3C829::AID-IJC11%3E3.0.CO;2-Y PMID: 9626349

36. Ceruti P, Principe M, Capello M, Cappello P, Novelli F. Three are better than one: plasminogen receptors as cancer theranostic targets. Exp Hematol Oncol. 2013; 2(1):12. doi: 10.1186/2162-3619-2-12 PMID: 23594883

37. Illemann M, Laerum OD, Hasselby JP, Thurison T. Urokinase-type plasminogen activator receptor (uPAR) on tumor-associated macrophages is a marker of poor prognosis in colorectal cancer. Cancer Med. 2014; 3(4):855–864. doi: 10.1002/cam4.242 PMID: 24889870

38. Chen D, Roda JM, Marsh CB, Eubank TD, Friedman A. Hypoxia inducible factors-mediated inhibition of cancer by GM-CSF: a mathematical model. Bull Math Biol. 2012; 74(11):2752–2777. doi: 10.1007/s11538-012-9776-3 PMID: 23073704

39. Fujimoto H, Sangai T, Ishii G, Ikehara A, Nagashima T. Stromal MCP-1 in mammary tumors induces tumor-associated macrophage infiltration and contributes to tumor progression. Int J Cancer. 2009; 125(6):1276–1284. doi: 10.1002/ijc.24378 PMID: 19479998

40. Hao W, Rovin BH, Friedman A. Mathematical model of renal interstitial fibrosis. Proc Natl Acad Sci USA. 2014; 111(39):14193–14198. doi: 10.1073/pnas.1413970111 PMID: 25225370

41. Acker T, Beck H, Plate KH. Cell type specific expression of vascular endothelial growth factor and angiopoietin-1 and -2 suggests an important role of astrocytes in cerebellar vascularization. Mech Dev. 2001; 108(1-2):45–57. doi: 10.1016/S0925-4773(01)00471-3 PMID: 11578860

42. Seghezzi G, Patel S, Ren CJ, Gualandris A, Pintucci G. Fibroblast growth factor-2 (FGF-2) induces vascular endothelial growth factor (VEGF) expression in the endothelial cells of forming capillaries: an autocrine mechanism contributing to angiogenesis. J Cell Biol. 1998; 141(7):1659–1673. doi: 10.1083/jcb.141.7.1659 PMID: 9647657

43. Bhowmick NA, Neilson EG, Moses HL. Stromal fibroblasts in cancer initiation and progression. Nature. 2004; 432(7015):332–337. doi: 10.1038/nature03096 PMID: 15549095

44. Hofland LJ, van der Burg B, van Eijck CH, Sprij DM, van Koetsveld PM. Role of tumor-derived fibroblasts in the growth of primary cultures of human breast-cancer cells: effects of epidermal growth factor and the somatostatin analogue octreotide. Int J Cancer. 1995; 60(1):93–99. doi: 10.1002/ijc.2910600114 PMID: 7529213

45. Kim Y, J W, F L, M O, Friedman A. Transformed epithelial cells and fibroblasts/myofibroblasts interaction in breast tumor: a mathematical model and experiments. J Math Biol. 2010; 61:401–421. doi: 10.1007/s00285-009-0307-2 PMID: 19902212

46. Mueller MM, Fusenig NE. Friends or foes—bipolar effects of the tumour stroma in cancer. Nat Rev Cancer. 2004; 4(11):839–849. doi: 10.1038/nrc1477 PMID: 15516957

47. Ronnov-Jessen L, Petersen OW, Koteliansky VE, Bissell MJ. The origin of the myofibroblasts in breast cancer. Recapitulation of tumor environment in culture unravels diversity and implicates converted fibroblasts and recruited smooth muscle cells. J Clin Invest. 1995; 95(2):859–873. doi: 10.1172/JCI117736 PMID: 7532191

48. Samoszuk M, Tan J, Chorn G. Clonogenic growth of human breast cancer cells co-cultured in direct contact with serum-activated fibroblasts. Breast Cancer Res. 2005; 7(3):R274–283. doi: 10.1186/bcr995 PMID: 15987422

49. Soon PS, Kim E, Pon CK, Gill AJ, Moore K. Breast cancer-associated fibroblasts induce epithelial-to-mesenchymal transition in breast cancer cells. Endocr Relat Cancer. 2013; 20(1):1–12. doi: 10.1530/ERC-12-0227 PMID: 23111755

50. Sadlonova A, Novak Z, Johnson MR, Bowe DB, Gault SR. Breast fibroblasts modulate epithelial cell proliferation in three-dimensional in vitro co-culture. Breast Cancer Res. 2005; 7(1):46–59.

51. Louzoun Y, Xue C, Lesinski GB, Friedman A. A mathematical model for pancreatic cancer growth and treatments. J Theor Biol. 2014; 351:74–82. doi: 10.1016/j.jtbi.2014.02.028 PMID: 24594371

52. Mallmann MR, Schmidt SV, Schultze JL. Macrophages in human cancer: Current and future aspects. PLoS ONE. 2012; 7(9):e45466.

53. Leek RD, Harris AL. Tumor-associated macrophages in breast cancer. J Mammary Gland Biol Neoplasia. 2002; 7(2):177–189. doi: 10.1023/A:1020304003704 PMID: 12463738

54. Hao W, Friedman A. The LDL-HDL profile determines the risk of atherosclerosis: a mathematical model. PLoS ONE. 2014; 9(3):e90497. doi: 10.1371/journal.pone.0090497 PMID: 24621857

55. Olson MW, Gervasi DC, Mobashery S, Fridman R. Kinetic analysis of the binding of human matrix metalloproteinase-2 and -9 to tissue inhibitor of metalloproteinase (TIMP)-1 and TIMP-2. J Biol Chem. 1997; 272(47):29975–29983. doi: 10.1074/jbc.272.47.29975 PMID: 9368077

56. Connolly BM, Choi EY, Gardsvoll H, Bey AL, Currie BM. Selective abrogation of the uPA-uPAR interaction in vivo reveals a novel role in suppression of fibrin-associated inflammation. Blood. 2010; 116 (9):1593–1603. doi: 10.1182/blood-2010-03-276642 PMID: 20466854

57. Chen D, Bobko AA, Gross AC, Evans R, Marsh CB. Involvement of tumor macrophage HIFs in chemotherapy effectiveness: mathematical modeling of oxygen, pH, and glutathione. PLoS ONE. 2014; 9(10): e107511. doi: 10.1371/journal.pone.0107511 PMID: 25295611

58. Enderling H, Chaplain MA, Anderson AR, Vaidya JS. A mathematical model of breast cancer development, local treatment and recurrence. J Theor Biol. 2007; 246(2):245–259. doi: 10.1016/j.jtbi.2006.12.010 PMID: 17289081

59. Liao KL, Bai XF, Friedman A. Mathematical modeling of Interleukin-35 promoting tumor growth and angiogenesis. PLoS ONE. 2014; 9(10):e110126. doi: 10.1371/journal.pone.0110126 PMID: 25356878

60. Shui YB, Wang X, Hu JS, Wang SP, Garcia CM. Vascular endothelial growth factor expression and signaling in the lens. Invest Ophthalmol Vis Sci. 2003; 44(9):3911–3919. doi: 10.1167/iovs.02-1226 PMID: 12939309

61. Lijnen HR, Van Hoef B, Ugwu F, Collen D, Roelants I. Specific proteolysis of human plasminogen by a 24 kDa endopeptidase from a novel Chryseobacterium Sp. Biochemistry. 2000; 39(2):479–488. doi: 10.1021/bi992014r PMID: 10631010

62. Paborsky LR, Tate KM, Harris RJ, Yansura DG, Band L. Purification of recombinant human tissue factor. Biochemistry. 1989; 28(20):8072–8077. doi: 10.1021/bi00446a016 PMID: 2690932

63. Curino A, Mitola DJ, Aaronson H, McMahon GA, Raja K. Plasminogen promotes sarcoma growth and suppresses the accumulation of tumor-infiltrating macrophages. Oncogene. 2002; 21(57):8830–8842. doi: 10.1038/sj.onc.1205951 PMID: 12483535

64. Lindhout T, Blezer R, Schoen P, Nordfang O, Reutelingsperger C. Activation of factor X and its regulation by tissue factor pathway inhibitor in small-diameter capillaries lined with human endothelial cells. Blood. 1992; 79(11):2909–2916. PMID: 1586738

65. Lwaleed BA, Francis JL, Chisholm M. Monocyte tissue factor levels in cancer patients. Saudi Med J. 2000; 21(8):722–729. PMID: 11423883

66. Ueno T, Toi M, Koike M, Nakamura S, Tominaga T. Tissue factor expression in breast cancer tissues: its correlation with prognosis and plasma concentration. Br J Cancer. 2000; 83(2):164–170. doi: 10.1054/bjoc.2000.1272 PMID: 10901365

67. Collen D, Wiman B. Turnover of antiplasmin, the fast-acting plasmin inhibitor of plasma. Blood. 1979; 53(2):313–324. PMID: 153773

68. Thielemann A, Baszczuk A, Kopczynski P, Kopczynski Z. High concentration of urokinase-type plasminogen activator receptor in the serum of women with primary breast cancer. Contemp Oncol (Pozn). 2013; 17(5):440–445.

69. Stillfried GE, Saunders DN, Ranson M. Plasminogen binding and activation at the breast cancer cell surface: the integral role of urokinase activity. Breast Cancer Res. 2007; 9(1):R14. doi: 10.1186/bcr1647 PMID: 17257442

70. Hildenbrand R, Schaaf A, Dorn-Beineke A, Allgayer H, Sutterlin M. Tumor stroma is the predominant uPA-, uPAR-, PAI-1-expressing tissue in human breast cancer: prognostic impact. Histol Histopathol. 2009; 24(7):869–877. PMID: 19475533

71. Benz CC. Impact of aging on the biology of breast cancer. Crit Rev Oncol Hematol. 2008; 66(1):65–74. doi: 10.1016/j.critrevonc.2007.09.001 PMID: 17949989

72. Kariko K, Kuo A, Barnathan E. Overexpression of urokinase receptor in mammalian cells following administration of the in vitro transcribed encoding mRNA. Gene Ther. 1999; 6(6):1092–1100. doi: 10.1038/sj.gt.3300930 PMID: 10455412

73. Hu Q, Lu YY, Noh H, Hong S, Dong Z. Interleukin enhancer-binding factor 3 promotes breast tumor progression by regulating sustained urokinase-type plasminogen activator expression. Oncogene. 2013; 32(34):3933–3943. doi: 10.1038/onc.2012.414 PMID: 22986534

74. Degnim AC, Brahmbhatt RD, Radisky DC, Hoskin TL, Stallings-Mann M. Immune cell quantitation in normal breast tissue lobules with and without lobulitis. Breast Cancer Res Treat. 2014; 144(3):539–549. doi: 10.1007/s10549-014-2896-8 PMID: 24596048

75. Kwon GY, Lee SD, Park ES. Mast cell and macrophage counts and microvessel density in invasive breast carcinoma-comparison analysis with clinicopathological parameters. Cancer Res Treat. 2005; 37(2):103–108. doi: 10.4143/crt.2005.37.2.103 PMID: 19956488

76. Blasi F, Vassalli JD, Dan K. Urokinase-type plasminogen activator: proenzyme, receptor, and inhibitors. J Cell Biol. 1987; 104(4):801–804. doi: 10.1083/jcb.104.4.801 PMID: 3031083

77. Estreicher A, Muhlhauser J, Carpentier JL, Orci L, Vassalli JD. The receptor for urokinase type plasminogen activator polarizes expression of the protease to the leading edge of migrating monocytes and promotes degradation of enzyme inhibitor complexes. J Cell Biol. 1990; 111(2):783–792. doi: 10.1083/jcb.111.2.783 PMID: 2166055

78. Strojan P, Budihna M, Smid L, Vrhovec I, Skrk J. Urokinase-type plasminogen activator (uPA) and plasminogen activator inhibitor type 1 (PAI-1) in tissue and serum of head and neck squamous cell carcinoma patients. Eur J Cancer. 1998; 34(8):1193–1197. doi: 10.1016/S0959-8049(98)00029-X PMID: 9849478

79. Quillin ML, Matthews BW. Accurate calculation of the density of proteins. Acta Crystallogr D Biol Crystallogr. 2000; 56(Pt 7):791–794. doi: 10.1107/S090744490000679X PMID: 10930825

80. Chorostowska-Wynimko J, Swiercz R, Skrzypczak-Jankun E, Wojtowicz A, Selman SH. A novel form of the plasminogen activator inhibitor created by cysteine mutations extends its half-life: relevance to cancer and angiogenesis. Mol Cancer Ther. 2003; 2(1):19–28. PMID: 12533669

81. Marino S, Hogue IB, Ray CJ, Kirschner DE. A methodology for performing global uncertainty and sensitivity analysis in systems biology. J Theor Biol. 2008; 254(1):178–196. doi: 10.1016/j.jtbi.2008.04.011 PMID: 18572196